An Experimental Study on Operability of Master-Slave Manipulator System using Human–in–the-Loop Type Simulator

Yosuke Tashiro[1], Hirofumi Ohtsuka[1], and Tomohiro Kawahara[2]

[1]*National Institute of Technology, Kumamoto College, 2659-2 Suya, Koshi, Kumamoto*
[2]*Kyushu Institute of Technology,2-4 Hibikino, Wakamatsu-ku, Kitakyushu-shi, Fukuoka,Japan*

Abstract. Double arm Master-Slave (M-S) manipulator has been attracted the attention of the robotics researchers today. The micro surgery is one of the big targets which M-S manipulator is expected to effectively perform. This paper describes about the human in the loop (HIL) simulator consisted of the prototype master manipulator and the virtual simulator of slave manipulator. Today, we have a challenge injecting drugs to a chick embryo's blood vessels that are enough cultured in an artificial eggshell. The M-S manipulator is expected to apply for such a work like a micro surgery, ex. catching a blood vessel and sticking a cylinder. The embryo is extremely sensitive so that M-S manipulator should have both high operability and high accuracy movement. To evaluate the M-S manipulator quantitatively, we develop the human in the loop (HIL) simulator. The simulator is consisted with the prototype master manipulator and the virtual slave manipulator.

1 Introduction

A surgery requires a lot of precise operation such as sewing a diseased part. In those operations, there necessarily exists some possibility that a human error makes heavy damage to patient. Therefore, it should be accepted for licensed doctors so that they are expected to grow their skills and institutional knowledge as sufficient high level. For the purpose of burden applied to both the surgeon and the patient, a surgery robot, such as "Da Vinci" has been developed and used. An operator (surgeon) can operate the slave manipulator through the master manipulator. The slave manipulator moves with a reduction of the master manipulator's motion. In addition, "Da Vinci" gives feedback force information from the slave to the master manipulator. However, its high cost has become an obstacle to widespread use.

Furthermore, when expanding the field of view, there is demand for surgical manipulation of the fine structure in the area of research related to the in-vivo technology. Many researchers try new drugs to chick eggs because it is quite cheap and ethically acceptable [1]. A chick egg is covered by hard eggshell, which pass oxygen into the inside of eggshell. Moreover it can't observe from outside [2]. Hence, Kawahara et al. have cultivated in artificial eggshell that has transparent body (Figure 1). The membrane thickness is 0.3 mm, the length is 40 mm, and the total volume of the cubic eggshell is approximately 50 ml [3].
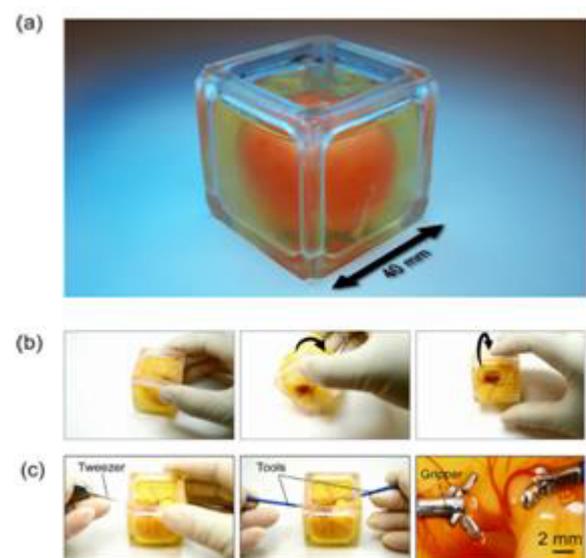

Figure 1. Developed cubic eggshell and the observation and manipulation of chick embryo.

It is clear that the chick embryo is delicate and the demand of robot is increasing. In this field, there are only few manipulators and these do not have enough operability. So, we have undertaken the M-S manipulator device which is capable of gripping the targeted blood vessel cultured in an artificial eggshell and on injecting a drug to it. For this

target, intricate structure such as "Da Vinci" is not required. It is desirable that can be deferred on the experiment table, so that we suggest proto-type 3 links manipulator shown in Figure 2. Master manipulator is smaller than slave one but both of manipulators have similarity shape 3 links. The slave manipulator successfully controlled to track the motion of master manipulator. However, operator's assessment is quite low for operability of master manipulator. So, we have undertaken the M-S manipulator device which is capable of gripping the targeted blood vessel cultured in an artificial eggshell and on injecting a drug to it. For this target, intricate structure such as "Da Vinci" is not required. It is desirable that can be deferred on the experiment table, so that we suggest proto-type 3 links manipulator shown in Figure 2. Master manipulator is smaller than slave one but both of manipulators have similarity shape 3 links. The slave manipulator successfully controlled to track the motion of master manipulator. However, operator's assessment is quite low for operability of master manipulator.
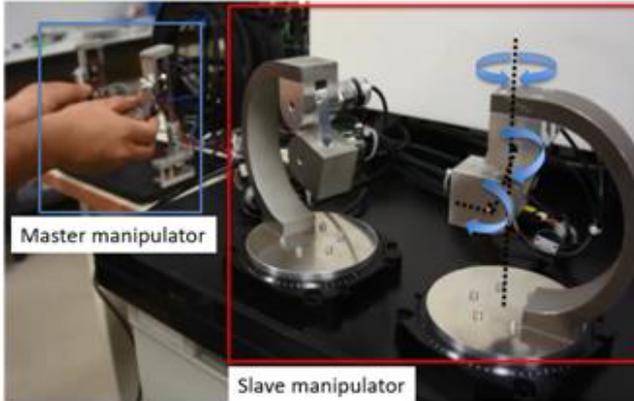

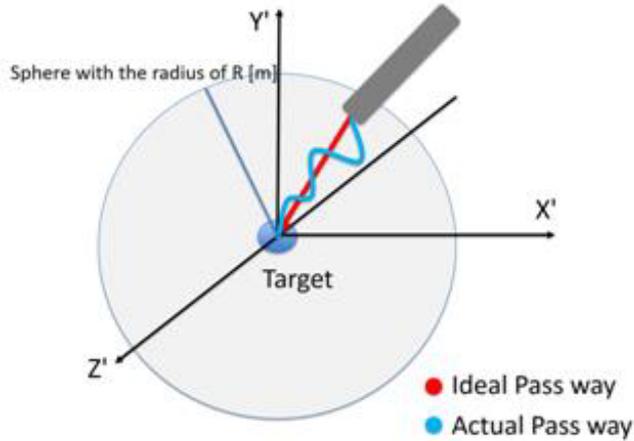**Figure 2.** Proto-type of master slave manipulator

Figure 3. Pass way of slave manipulator tip position

2 Human-in-the-Loop type Master-Slave Manipulation Simulator

Main objective of this study is improving the operability of M-S manipulator shown in Figure 2. To design the high operability M-S manipulator system, the quantitative index for operability is required. Since the performance of M-S manipulator system depends on the movement of the slave manipulator's end effect joint, let us focus on the tip position of end effector of slave manipulator.
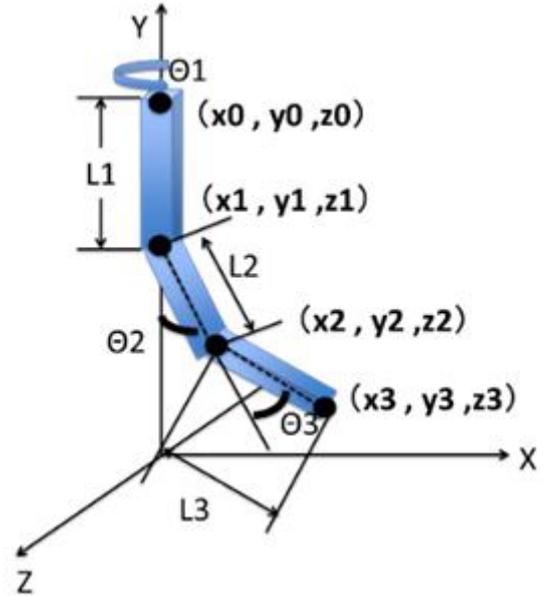

Figure 4. Physical model of the slave manipulator

When the 3 dimensional coordinate denoted in Figure 3, we consider the evaluation space as a sphere of the radius R[m] with the centre point as target position. And an orthogonal coordinate space, with origin as target position, is defined as shown in Figure 3. After the tip of the slave manipulator has entered the sphere space, its trajectory becomes an ideal pass way shown as red line in Figure 3 for the best operability. For less operability case, its trajectory shows the fluctuation around the ideal pass way such as "Actual Pass way" described by blue line.

2.1 Forward kinematics of manipulator

The slave manipulator has 3 links shown in Figure 2, so its schematic diagram can be described by Figure 4. The origin of orthogonal coordinate is different from Figure 3. Here, we define the arms from the top, arm 1, arm 2 and arm 3. And the fasten position is given as follows.

$$(x0, y0, z0) = (0, Y0, 0) \tag{1}$$

$$(x1, y1, z1) = (0, Y0 - L1, 0) \tag{2}$$

Now calculation is below. (Each arm's rotation is $\theta1$, $\theta2$ and $\theta3$.)

$$x2 = L2\sin\theta2 * \cos\theta1 + x1 \tag{3}$$

$$y2 = y1 - L2\cos\theta2 = Y0 - L1 - L2\cos\theta2 \tag{4}$$

$$z2 = L2\sin\theta2 * \sin\theta1 + z1 \tag{5}$$

In the end, the coordinates of the tip position is calculated as below.

$$x3 = x2 + L3 * sin(\theta2 + \theta3) * cos\theta1$$

$$= \{L2 sin\theta2 + L3 \ sin(\theta2+\theta3)\} * cos\theta1 \qquad (6)$$

$$y3 = y2 - L3 * cos(\theta2 + \theta3)$$

$$= Y0 - L1 - L2 cos\theta2 - L3 cos(\theta2+\theta3) \qquad (7)$$

$$z3 = z2 + L3 * sin(\theta2 + \theta3) * sin\theta1$$

$$= \{L2 \ sin\theta2 + L3 * sin(\theta2+\theta3) \} * sin\theta1 \qquad (8)$$

Now, let us denote a displacement between the tip position and the target position as:

$$d = \sqrt{p_x^2 + p_y^2 + p_z^2} \qquad (9)$$

where (p_x, p_y, p_z) is a coordinate of tip position. The coordinate of tip position (p_x, p_y, p_z) can be obtained from eq.(6)-(8) by use of the coordinate transformation matrix among those orthogonal coordinate space.
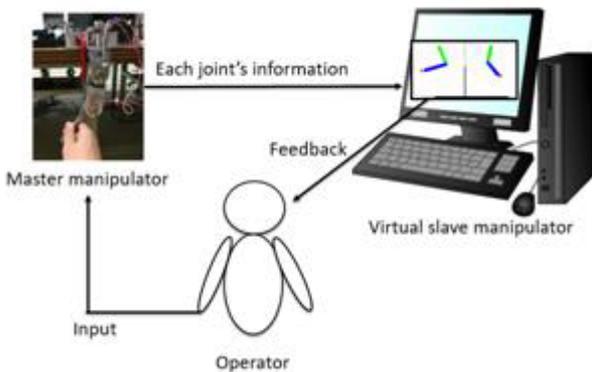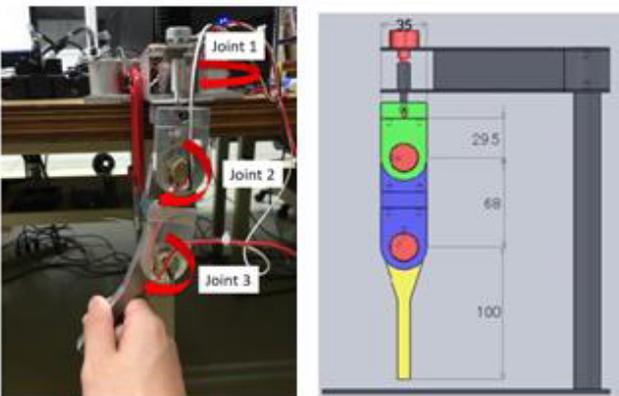

Figure 5. Human in the loop simulator

Figure 6. Overview of the master manipulator

2.2 Simulator

To evaluate the operability of M-S manipulator system, we built an experimental context which is shown as Figure 5. The mechanical design of master manipulator (Figure 6) has been done with a use of 3D-CAD software "Solid

works". Rotational angles for all joints of master manipulator can be detected by potentiometer attached with the each axis. The voltage signals from them are input to the computer through the AD/DA converter interface board. Specs of the equipment are shown in Table 1, Table 2 and Table 3.
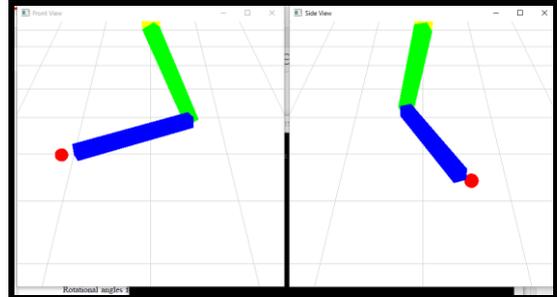

Figure 7. User interface of virtual slave manipulator

Table 1. PC Specs

Processor	Intel Core i5 - 4460 CPU 3.20GHz
RAM	16.0GB
Operating System	Windows 10 Pro 64bit

Table 2 D/A BOARD Specs

Model number	PEX-340416
Channels number	4 channels
Output voltage	? 0V
Resolution	16bit

Table 3 A/D board specs

Model number	PEX-361216
Channels number	Single ended:16 channels
	Differencial: 8 channels
Maximum sampling time	1 MSPS
Input voltage	? 0V

The operator can see the animation image of the virtual slave manipulator on the monitor screen (Figure 7). At the same time, the operator can handle and operate the master manipulator to achieve a task such as positioning the tip position to the target position. The motion of the slave manipulator is calculated in the computer by using the forward kinematics equations (1) - (9) as mentioned above. The tip positions of each link can be calculated, then wire-flame model are repeatedly drawn on the monitor screen. There will be two windows from the front and side viewpoint because it is generally hard to get the position of the target with only one viewpoint even it is a 3D image.

3 Quantitative evaluation for operability

3.1 The time for ending a work

Now, we propose the following 3 type of the quantitative index. The time to end an assigned work is one of the important factors showing the operability. It is clear that the time for ending tasks becomes longer the case of less operability than the case of high operability.

3.2 Average Absolute Error (AAE)

In the experiment for assessment of the operability, a subject is ordered to control the virtual S-manipulator which is shown on the screen through the M-manipulator. The system shows the target as moving red ball on the screen in real-time. The target moves linearly from the previous target position to next target position.

Then N_i second later (i = 0, 1, 2: i is the task number), the target will arrive the target position. After the target stops moving, the target can take next process when the tip position is near the goal. Now, we define the time series target position's x, y and z coordinate of axis as $X_t(t)$, $Y_t(t)$ and $Z_t(t)$. And the time series tip position's x, y and z coordinate of axis as $X(t)$, $Y(t)$ and $Z(t)$. Furthermore we suggest a parameter AAE to measure how a user could follow the target position as the equation (10).

$$AAE_i = \sum_{i=0}^{N_i} \frac{\sqrt{(X_t(t) - X(t))^2 + (Y_t(t) - Y(t))^2 + (Z_t(t) - Z(t))^2}}{N_i}$$
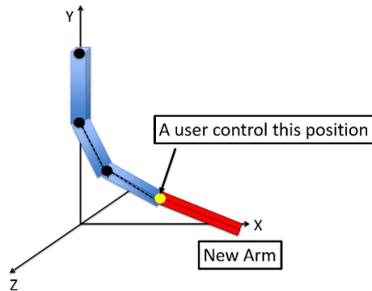
(10)

Figure 8. An arm downing operability

3.3 Vibration rate

Taking into the account that how the manipulator is accuracy near the target, we adopt an assessment value vibration rate ζ, which is defined as follow.

$$\zeta = P_l / R$$

(11)

When the tip position of the slave manipulator is in R [m] to the target, by recording the tip position, we can measure the approximate length of actual pass way P_l [m] as

$$P_l = \sum \sqrt{\Delta P_x^2 + \Delta P_y^2 + \Delta P_z^2}$$

(12)

where $\Delta P_* = p_*(t + \Delta_g) - p_*(t)$, $*$ is x, y or z. and Δ_g denotes the sampling period of simulator.

4 Experimental results

To certify the effectiveness of the parameters, we consider two types of master manipulator. We call these two manipulators the original type and less operability type. The second type is extended length of 3rd arm as shown in Figure 8.

4.1 Binomial test

A subject is ordered adjusting the tip position to a red point shown in the window. The target position moves linearly from the previous target position to the next target position in constant velocity. There are 3 target position and we call the order from the target position to position as work I. (I = 1, 2, and 3: number of target position.) Mainly we assess the 3 parameters that already defined section 3 however comparing the single value is not effective. Because the result basically has a dispersion caused by human controlling. For that reason, we need to measure how often a user get a value over a standard value. In this time, we use the each median value that is calculated from the designed M-manipulator at each of subject. Figure 9 is a binomial distribution with parameters 80 (number of experiment) and 0.5 (probability of occurrence).

4.2 Result

We have done experiment 20 times to 4 subjects and calculated the parameters of each work with new arm and without new arm. Then we collect the numbers how many time the data over the median value as Table 4. The number how many time the parameter over and below the median value are shown as good and bad. The median value is calculated individually from the experiments with the original M-manipulator.

Table 4. Result of experiment

	time1		time2		time3	
	good	bad	good	bad	good	bad
Subject A	13	7	12	8	7	13
Subject B	2	18	8	12	6	14
Subject C	10	10	6	14	11	9
Subject D	3	17	7	13	10	10
sum	28	52	33	47	34	46
Percentage	0.002407348		0.026361786		0.036441293	

	Vibration rate 1		Vibration rate 2		Vibration rate 3	
	good	bad	good	bad	good	bad
Subject A	7	13	7	13	1	19
Subject B	0	20	5	15	1	19
Subject C	7	13	5	15	6	14
Subject D	15	5	13	7	17	3
sum	29	51	30	50	25	55
Percentage	0.004316624		0.00733826		0.000300609	

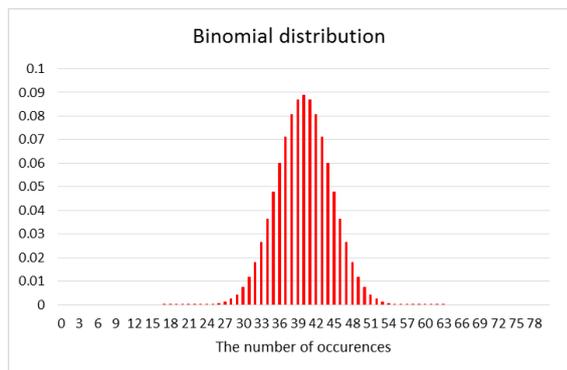|	AAE1		AAE2		AAE3	
	good	bad	good	bad	good	bad
Subject A	7	13	16	4	6	14
Subject B	5	15	9	11	8	12
Subject C	2	18	1	19	10	10
Subject D	8	12	11	9	6	14
sum	22	58	37	43	30	50
Percentage	2.24073E-05		0.071194185		0.00733826	

Figure 9. Binominal distribution of 80 time operation

The percentage, how many time occur the result over standard value below binominal distribution, is the percentage in the Table 4 [5].

5   Conclusion

We set the significance level as 0.05 for one side binominal test and the Figure 9 shows binominal distribution [6]. The parameters, time1, time2, time3, vibration rate1, vibration rate2, vibration rate3, AAE1 and AAE3, meet one side binominal test. AAE2 doesn't meet the one side binominal test however AAE2 meets the both side binominal test. Taking into account these result, we conclude the parameters are enough effective to assess the operability.

Consequently, we will quantitatively improve the operability of master manipulator based on these parameters.

References

1. Huang W, Arai F, Kawahara T (2015) Egg-inCube: Design and Fabrication of a Novel Artificial Eggshell with Functionalized Surface. PLoS IONE 10 (3);e0118624. Doi:10. 1371 / journal.pone.0118624
2. Tsai T, Yang JM, Lai CW, Cheng YH, Lin CC, Yeh CW (2006) Characterization and adsorption prop-erties of eggshells and eggshell membrane. Bioresour Technol 97: 488–493. PMID: 15896954
3. Wenjing Huang, Fumihito Arai, Tomohiro Kawahara(2015); Inducing blood vessel formation using cubic eggshell with patterned surface. IEEE 15872410 DOI: 10.1109/MHS.2015.7438255
4. ISO 9241-11:1998(en), Ergonomic requirements for office work with visual display terminals (VDTs) — Part 11: Guidance on usability; https://www.iso.org/obp/ui/#iso:std:iso:9241:-11:ed-1:v1:en(Access 05/10/2016)
5. Kei Takeuchi, Kazutake Fuhino (1981); Binomial Distribution and Poisson distribution. Japan University of Tokyo Press
6. Jakob Nielsen, Toshikazu Shinohara(translator): Usability Engineering(2002), Tokyo Denki University Luigi T.De Luca, *Propulsion physics* (EDP Sciences, Les Ulis, 2009) . F. De Lillo, F. Cecconi, G. Lacorata, A. Vulpiani, EPL, **84** (2008)